POLITECNICO DI TORINO
Repository ISTITUZIONALE

Throughput Optimization in a Tunable Subcarrier-based Coherent PON

Original
Throughput Optimization in a Tunable Subcarrier-based Coherent PON / Arnaout, S., Alzoubi, S., Rahman, M.A., Gaudino, R.. - (2026), pp. 1-6. (2026 IEEE International Conference on Communications, ICC 2026 Glasgow (UK) 24-28 May 2026) [10.1109/icc59461.2026.11587709].

Availability:
This version is available at: 11583/3013798 since: 2026-07-31T11:32:01Z

Publisher:
IEEE

Published
DOI:10.1109/icc59461.2026.11587709

Terms of use:

This article is made available under terms and conditions as specified in the corresponding bibliographic description in the repository

Publisher copyright
IEEE postprint/Author's Accepted Manuscript

©2026 IEEE. Personal use of this material is permitted. Permission from IEEE must be obtained for all other uses, in any current or future media, including reprinting/republishing this material for advertising or promotional purposes, creating new collecting works, for resale or lists, or reuse of any copyrighted component of this work in other works.

(Article begins on next page)

14 November 2026

Throughput Optimization in a Tunable Subcarrier-based Coherent PON

Sandra Arnaout,[1,*] Safana Alzoubi,[2] Md Arifur Rahman,[1] and Roberto Gaudino [2]
[1]IS-Wireless, ul. Pulawska 45b, 05-500 Piaseczno, Poland
[2]Dipartimento di Elettronica e Telecomunicazioni, Politecnico di Torino, Torino, Italy
[*]s.arnaout@is-wireless.com

***Abstract*—In the Very High Speed Passive Optical Network (VHSP-PON) initiative, ITU-T is currently analyzing which physical-layer transmission solution will be the best for next-generation 200G PON, and one of the possible options under study is digital subcarrier-based coherent PON (DSC-PON). Under this scenario, we present in this paper a study on the heuristic optimization of dynamic time and subcarrier allocation in DSC-PON, under realistic assumptions in terms of limited bandwidth and limited laser tunability at the optical network unit (ONU) side receiver. In this paper, we propose a heuristic Greedy Graph Coloring Algorithm (GGCA) to solve subcarriers (SCs) and timeslot allocation problems that map the traffic generated by the users. Moreover, we also consider tunability of the ONU that switches the subcarrier block in different time-frames. Consequently, our proposed GGCA algorithm follows such tunability constraints of the local oscillator and provides allocation of the SCs to maximize the throughput of DSC-PON. We evaluate the performance of our proposed GGCA algorithm with different tunability times and show that it is improved approximately (35%) of throughput with full tunability compared to slow tunability.**

***Index Terms*—Passive optical network, optical network unit, subcarrier allocation, greedy graph coloring algorithm, throughput.**

I. Introduction

ITU-T is currently investigating on which transmission solutions will be selected for the next generation of optical access networks based on PON architectures, after the release in 2023 of the final ITU-T Recommendation for 50G-PON. In particular, in the the Very High Speed PON (VHSP) initiative [1], [2] several modulation formats are currently under analysis as candidates for a future 200G-PON Recommendation targeting 200 Gbps bit rate, symmetrically in both downstream (DS) and upstream (US) PON directions. The request for such high bit rate in PON access is driven by some expected near-term trends, such as the massive adoption of fronthauling directly over PON (see for instance [3] in the section on Functional Split 7.2x). The technical challenges at the physical layer are still quite open, as discussed in [4], which examines the debate between continuing with intensity-modulation direct detection (IMDD) and transitioning to higher-order modulation combined with coherent transmission. Specifically, the authors in [4] analyze DSP countermeasures for IMDD challenges, such as chromatic dispersion and bandwidth limitations at higher data rates, and, in contrast, investigate coherent DSP adaptations to PON dynamics, such as burst-mode reception, as well as system simplifications aimed at preserving the cost effectiveness of PON. One of the possible candidates for 200G-PON in VHSP is a PON architecture based on digital subcarrier (SC) multiplexing at the transmitter side and coherent detection at the receiver, indicated in the following as digital subcarrier-based coherent PON (DSC-PON).

Several papers have been recently published on coherent transmission in PON, including DSC-PON, in which enabling technologies, use cases, and experimental demonstrations are extensively discussed. The interested reader can refer for instance to the one proposed in [5], [6] for the so-called C-PON initiative led by CableLabs, and involving today several partners, as shown in [7]. In DSC-PON, multiple subcarriers are digitally generated within the transmitter's digital signal processing (DSP) to modulate the same optical wavelength, and are correspondingly digitally demultiplexed at the receiver through parallelization of the DSP modules, in contrast to single-carrier coherent PON systems. It is well known that one of the advantages of DSC-PON employing single-carrier coherent transceivers is that the limited bandwidth of the ONU only restricts the number of adjacent subcarriers it can receive, rather than the system capacity as a whole. The usage of the adjacent SCs allows us to use the bandwidth more efficiently, which can significantly improve the spectrum utilization. Therefore, the authors in [8] propose an architecture and algorithm for SCs allocation and demonstrate multiple access in time/frequency domain (TFDMA)-based coherent PON in real-time. Similarly, Zhang et al. propose burst mode transmission and reception of the DSP process of 100 Gb/s coherent TFDMA PON [9]. As is known, coherent PON brings high-capacity, long-reach, and flexible PON by leveraging coherent detection and DSP, surpassing traditional detection and modulation of the PON systems. Motivated by the benefits of coherent PON, in this paper we address the problem of of SCs allocation and propose a Greedy Graph Coloring algorithm (GGCA) to dynamically allocate the timeslots and SCs. The main contribution of this paper can be highlighted as follows:

- Firstly, we formulate the problem of dynamic subcarrier and timeslot allocation in DSC-PON as an integer linear programming (ILP) model that accounts for varying user traffic demands and ONUs tunability constraints.
- Secondly, we propose GGCA to optimally allocate the

SCs considering different tunability times of all ONUs oscillators. Moreover, the proposed GGCA follows the tunability threshold and skips the allocation of SCs in that dedicated tuning frames.

- Thirdly, we conduct extensive simulations to evaluate the performance of the proposed GGCA by considering three cases: (i) fast tunability, where the ONU's central frequency can shift to a different frequency within the burst preamble duration; (ii) slow tunability, where the tuning time spans an integer number of upstream frames (k frames in general); and (iii) the static-laser case (which will be taken as a benchmarking reference), in which each ONU employs a fixed laser that cannot be tuned, and thus it can be assigned only a static subcarrier position from first index of SC to adjacent three other SCs.
- Finally, we also investigate the consequences of realistic tunability time of the laser (i.e., the time needed to change the SCs subset by physically changing the ONU laser central frequency).

The paper is organized as follows. Section II describes the DSC-PON system model and physical considerations, followed by the formulation of the SC and timeslot allocation problem along with the corresponding optimization objective. Section III presents the proposed heuristic algorithm developed to address the allocation problem. The simulation environment, results, and discussion are provided in detail thereafter in Section IV. Finally, the paper concludes with a summary of key findings.

II. System Model and Problem Definition

This section presents the system-level conceptual scheme of the DSC-PON upstream transmission, as illustrated in Fig. 1, where each ONU has limited bandwidth, employs a distinct modulation format, and is equipped with a tunable laser with subcarrier-level granularity. A 16-subcarrier uplink system is considered with a sufficient guard-band between the SCs to avoid inter-subcarrier interference, as shown in Fig. 1 inset (B). Consequently, ONUs share both time and frequency domains according to the allocation map determined by the OLT, similar to the example illustrated in Fig. 1 inset (A).

In the considered DSC-PON system, resource allocation is constrained by ONU physical limitations, including bandwidth, laser tunability, and modulation capability. ONU bandwidth is determined by the number of adjacent subcarriers (SCs) it can use within a timeslot. Laser tunability defines when retuning is needed, i.e., when an ONU must shift from its current SC block to another wavelength within the system bandwidth. During the tuning time, which may be fast, slow, or static, the ONU cannot transmit. If DSCM is adopted in large-scale PON deployments, laser tunability enables differentiation among user classes according to their contribution to ONU cost. Specifically, low-cost ONUs serving residential services may employ slow-tuning lasers, whereas ONUs supporting fronthaul services can use fast-tuning lasers to mitigate tuning delays. The tunability mechanisms of the ONU laser can be seen in Fig. 2 that we can allocate one or more adjacent SCs in different timeslots within the same timeframe. In the tunability case, if the ONU has 4 tuning frames no SCs will be allocated to transmit the packets. Finally, the supported modulation format depends on the ONU's optical distribution loss: ONUs with lower loss can employ higher-order modulation formats while maintaining the required bit error rate (BER), whereas ONUs with higher loss are restricted to lower-order modulation schemes. In this study, the modulation formats considered for ONUs include quadrature phase-shift keying (QPSK), 8-level quadrature amplitude modulation (8-QAM), and 16-level QAM (16-QAM), depending on their respective optical distribution losses.

TABLE I: Mathematical Notations

Notation	Description
M	Total number of ONUs
$\mathcal{I}$	Number of ONUs in transmission mode
K	Number of subcarriers in the system
N	Number of blocks in the system
B	Block size
T	Number of timeslots in each frame
F	Number of frames
i	Index representing the i^{th} ONU
s	Index representing s^{th} subcarrier
t	Index representing the t^{th} timesolt
b	Index representing the b^{th} block
D_i	Traffic demands of the i^{th} ONU
SC_{max}	Maximum allowed SCs for i^{th} ONU
r_i	Supported data rate of the i^{th} ONU
$x_{i,s,t}$	Binary variable indicating if the i^{th} ONU is allocated to subcarrier s and timeslot t
$y_{i,b}$	Binary variable indicating if the i^{th} ONU is allocated to block b
z_i	Binary variable indicating if the i^{th} ONU changes its assigned block

Building on these physical considerations, we propose an optimization algorithm for subcarrier and timeslot allocation that is aware of each ONU's physical state. The description of the notations used in the problem formation and constraints is summarized in Table I. We start by formulating the SC and timeslot assignment to ONUs as a linear programming problem with the objective of maximizing the overall system throughput, as defined in Eq. 1. The proposed algorithm considers several input parameters, including the number of ONUs (M) and, in particular, the subset $\mathcal{I}$ representing the ONUs currently in transmission mode rather than in tuning mode. Additional parameters include the number of subcarriers (K), and the number of timeslots (T) in each 125 μs frame. We define $x_{i,s,t}$ as a binary decision variable indicating whether the i^{th} ONU is assigned to the s^{th} subcarrier and t^{th} timeslot. Each ONU operates at a data rate r_i, which depends on its supported modulation format. The optimization problem can be formulated as:

$$\max \sum_{i \in \mathcal{I}} \sum_{s=1}^{K} \sum_{t=1}^{T} r_i x_{i,s,t} \tag{1}$$

We assume that the total system bandwidth, comprising K

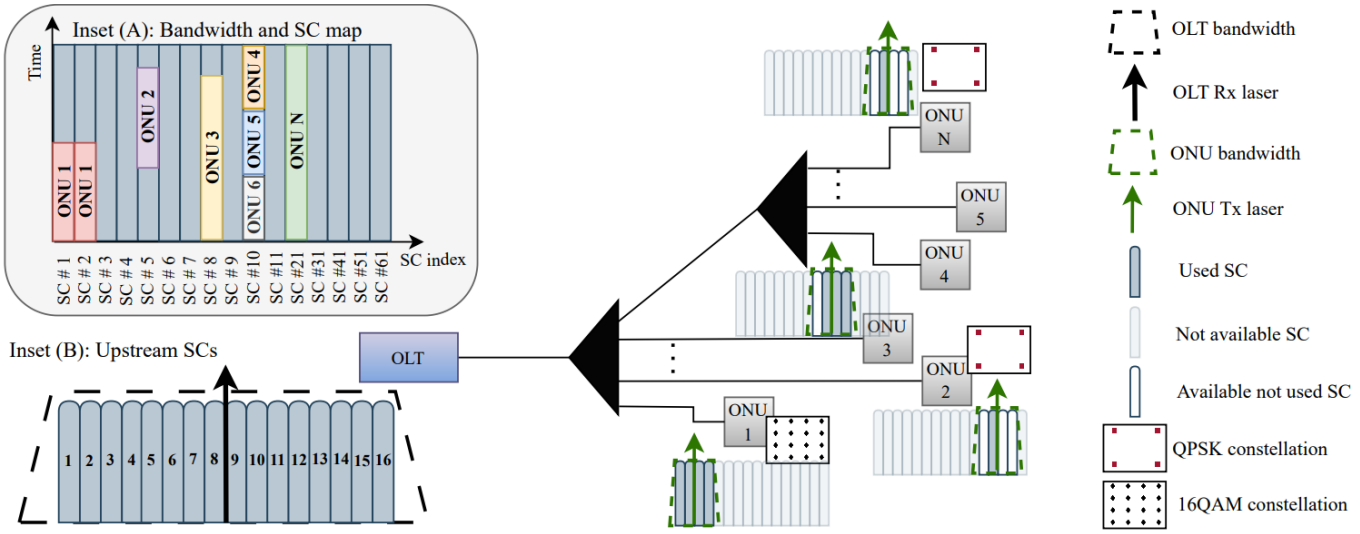

Fig. 1: System model of a DSC-PON employing limited-bandwidth ONUs and various modulation formats. Inset (A) illustrates an example of SC and timeslot allocation mapping, while Inset (B) depicts the total upstream SCs at the OLT.

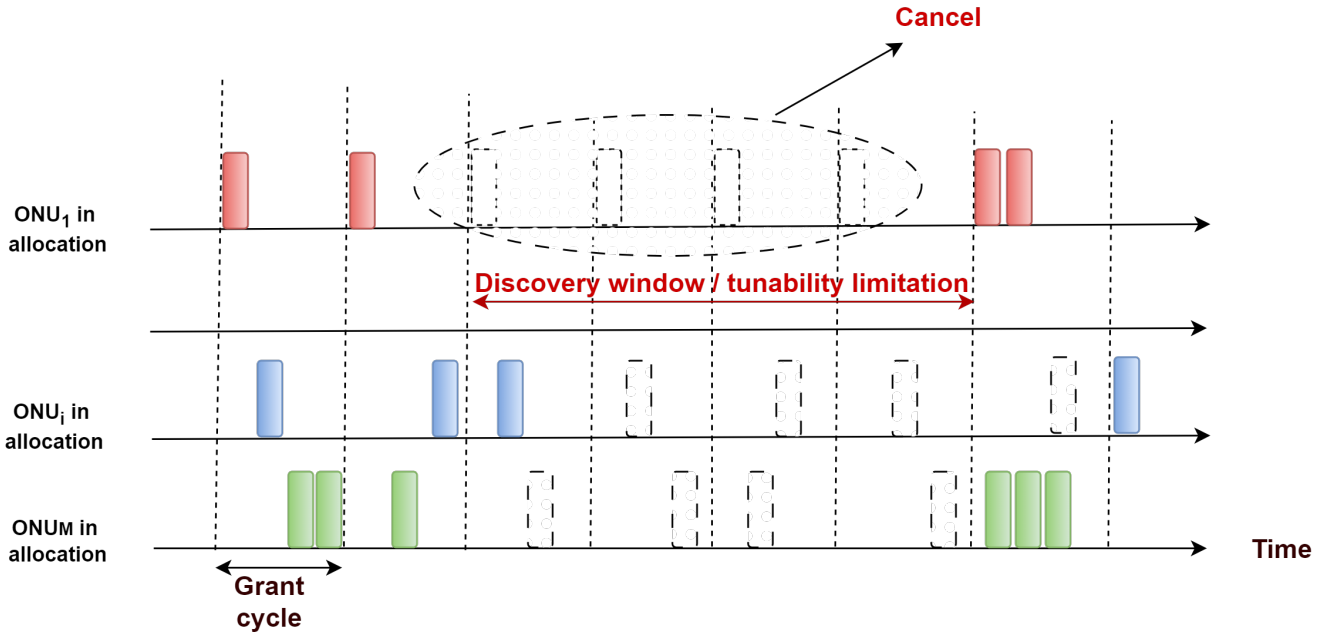

Fig. 2: An example of Tunability of ONU oscillator.

SCs, is divided into N blocks (SC subsets), each consisting of B adjacent SCs. A change in block indicates that the ONU must retune its TX laser to enable data transmission. Consequently, the blocks are generated using a sliding window of size B with a stride of one (i.e., one SC). The binary variable $y_{i,b}$ denotes whether ONU i is assigned to block b, while z_i indicates whether ONU i changes its block. The decision and auxiliary binary variables are defined as follows:

$$x_{i,s,t},\ y_{i,b},\ z_i \in \{0,1\}, \quad \forall i,\ s,\ t,\ b \tag{2}$$

The problem constraints are defined as follows: the first constraint in (3) ensures that ONUs in the tuning state are not assigned any resources:

$$x_{i,s,t} = 0, \quad \forall i \notin \mathcal{I},\ \forall s,\ \forall t \tag{3}$$

The second constraint in (4) enforces that each ONU is allocated to only one block:

$$\sum_{b=1}^{K} y_{i,b} \leq 1, \quad \forall i \in \mathcal{I} \tag{4}$$

The third constraint in (5) ensures that the allocated SCs

remain within the assigned block:

$$x_{i,s,t} \leq \sum_{b:\, s \in B_{\text{map}}(b)} y_{i,b}, \quad \forall i \in \mathcal{I},\ \forall s,\ \forall t \tag{5}$$

The fourth constraint in (6) ensures that when an ONU changes its block (corresponding to a change in the TX laser position and entry into the tuning phase), it is not transmitting and therefore is not allocated any resources:

$$x_{i,s,t} \leq 1 - z_i, \quad \forall i \in \mathcal{I},\ \forall s,\ \forall t \tag{6}$$

Additionally, the constraint in (7) ensures that each ONU can have one or more (up to 4) adjacent subcarriers in each frame

$$\sum_{i \in \mathcal{I}} x_{i,s,t} \leq SC_{max}, \quad \forall i,\ \forall t \tag{7}$$

Constraint in (8) ensures that the total number of resources allocated to each transmitting ONU does not exceed its traffic demand, where traffic demands is D_i in bits and therefore, divided by the ONU rate r_i and the slot duration to determine the corresponding number of required timeslots.

$$\sum_{s=1}^{K} \sum_{t=1}^{T} x_{i,s,t} \leq \left\lceil \frac{D_i}{r_i \times slot_duration} \right\rceil, \quad \forall i \in \mathcal{I} \tag{8}$$

Finally, the last constraint in (9) guarantees that ONUs in transmission mode do not share the same subcarrier and timeslot within a given frame:

$$\sum_{i \in \mathcal{I}} x_{i,s,t} \leq 1, \quad \forall s,\ \forall t \tag{9}$$

The ILP complexity is exponential in terms of number of ONUs and number of blocks. In our problem formulation, let M be the number of ONUs and N the number of subcarriers blocks, so the ILP will contains M * N binary variables and since the ILP is NP-hard, the worst-case complexity is grow as $O(M^N)$. Although ILP provides an optimal solution, it has scalability limitations because it grows exponentially. To that end, we propose solving it using a heuristic that provides near-optimal throughput. More details are listed in the following section.

III. The Proposed Greedy Graph Algorithm for Subcarriers Allocation

In this paper, we propose a GGCA to solve SCs and timeslot allocation problem in a coherent PON. Initially, the available subcarriers are divided into blocks of four to track the tunability of ONUs. The allocation of these blocks follows a demand-aware strategy, where ONUs with higher traffic demands are prioritized. For each ONU, the algorithm computes the required resources (expressed as subcarriers (SCs) × timeslots (TS)) based on its demand and supported modulation data rate. In each timeslot, GGCA attempts to find available (free) subcarriers within the ONU's assigned block and allocates them according to their demands. Once a subcarrier is assigned, it is marked as busy (or taken) for that timeslot to avoid collisions with other ONUs. This process continues until all demands are satisfied or the frame is fully occupied. At the end of each frame, ONU states are updated, including remaining demand and whether block retuning is needed. Retuning is triggered only when the demands cannot be met within the current block, and switching is expected to improve throughput. GGCA is modeled as an undirected graph G = (V, E) [10], where vertices represent ONUs and edges indicate assignment conflicts. The full procedure is given in Algorithm 1. From a computational perspective, lets denote M is the number of ONUs, E is the number of conflict edges and K is the number of subcarriers, then the computational complexity is $O(E + M.K)$ in the worst case, because each ONU is processed once per frame, and for each ONU, the proposed algorithm checks up to K available subcarriers and verifies conflicts only with neighboring ONUs.

IV. Simulation Results

The simulation results presented in the following section were obtained using a system-level simulator, which is a Python-based simulator. Concerning the traffic model, we assume that we have three clusters of ONUs, where each ONU's cluster supports one modulation type (i.e., ONUs in cluster one support 16QAM), and 3% of ONUs generate fronthauling (FH) traffic, while the rest have normal data traffic. ONUs traffic models are represented by a simple Poisson process [11], which is widely used to represent stochastic traffic behavior of the network. Packet inter-arrival times are generated according to an exponential distribution, while packet sizes are uniformly distributed between 64 and 1518 bytes, corresponding to standard Ethernet frame sizes [12]. The number of simulated packets is chosen big enough to reach a saturation in the network, and the average throughput performance is calculated based on that. The duration of each frame was assumed to be 125µs; each frame is divided into 125 timeslots, so the duration of one timeslot is assumed to be 1µs. For this architecture, we have performed the performance evaluation of the average throughput for all ONUs across all 500 simulated frames. Three scenarios are considered here regarding the tuning capabilities: no-tuning, fast, and slow tuning. A summary of the key system parameters and their typical values that we use to evaluate our simulation is listed in the Table II below:

Figure 3 illustrates the performance for three cases; no-tuning, fast and slow tuning as a function of the traffic load offered. Overall, we can observe that throughput increases with the offered load until it reaches high load levels, up to a point where it starts to saturate in significantly different ways, depending on the tunability options. In particular, in the fast tuning scenario, ONUs can freely switch between subcarrier blocks to satisfy their demands without any blocking, resulting in the highest throughput among the three cases. In contrast, the no-tuning case yields the lowest throughput because ONUs are constrained to a fixed subcarrier block across frames. In this case, once an ONU is assigned a block, it cannot switch to another block in subsequent frames, which limits its ability

Algorithm 1 The proposed GGCA

1: **Initialization**: Create a matrix for assigning SCs and timeslots. Mark all SCs as free at the beginning of the assignment.
2: **Sorting**: Order ONUs by priority
3: **Edges (Conflict Definition)**: Make an edge between two vertices (ONUs) if these two ONUs can't be assigned the same subcarrier in the same timeslot. This encodes the collision constraints between ONUs.
4: **Coloring (SCs allocation)**: For each ONU (vertex) in the priority order, find the first available color (SC) in its block that don't conflict with already colored vertices.
5: **Assignment**: Assign these subcarriers and mark them as busy/taken for the current timeslot
6: **Update**: Update the ONU's mapping state for the current frame.
7: **Iteration**: Repeat the allocation process until all ONUs have been assigned resources or no free subcarriers/timeslots remain.

TABLE II: Simulation parameters

Parameter	Typical Value
Number of ONU's cluster	3
Number of ONUs	60
Number of frames	500
Number of subcarriers	16
Frame duration	125μs
Timeslot duration	1μs
Number of timeslots per frame	125
Packet length	64-1518 $bytes$
Data peak rate	5 Gbps
Fronthauling peak rate	22.5 Gbps
Modulation types	16QAM, 8QAM, QPSK
Maximum supported rate for 16QAM	25 Gbps (for 16 SCs)
Maximum supported rate for 8QAM	18.75 Gbps (for 16 SCs)
Maximum supported rate for QPSK	12.5 Gbps (for 16 SCs)

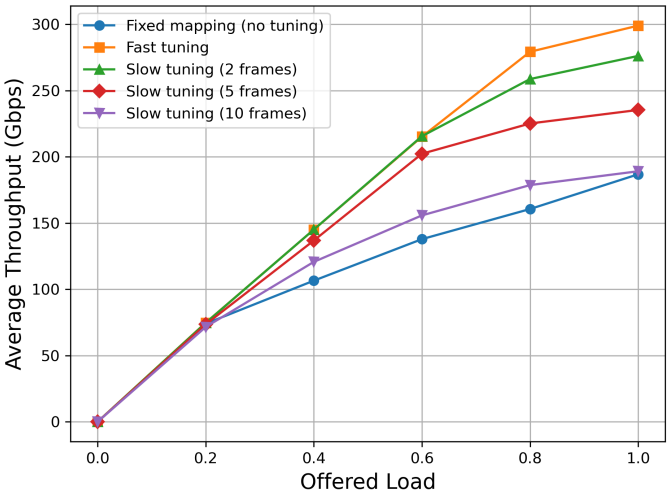

Fig. 3: Throughput as a function of offered load.

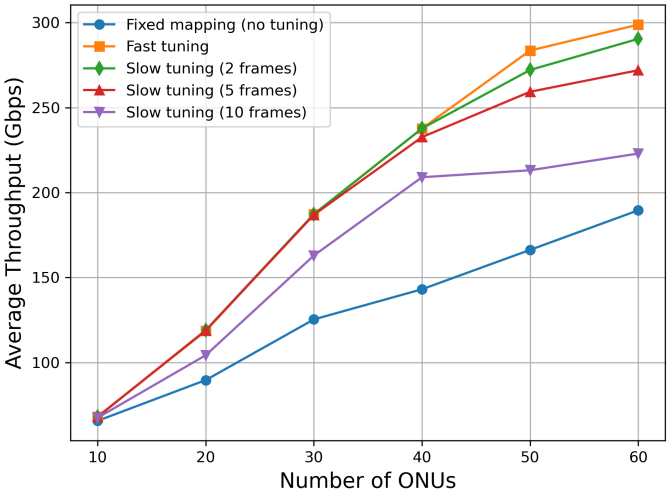

Fig. 4: Throughput as a function of number of ONUs.

to fully utilize available resources. For the slow tuning case, simulations were performed with different numbers of tuning frames. We observe that the fewer the tuning frames, the higher the throughput. This is because an ONU in the tuning state remains without allocated resources for a shorter period. For example, with tuning requiring 5 frames, an ONU will remain unallocated for 5 frames while tuning, after which it can transmit both its newly arrived traffic and the buffered traffic accumulated during the tuning period.

Figure 4 shows throughput versus the number of ONUs (10–60), under three tuning cases (no-tuning, fast, and slow) with the offered load fixed at 1 to represent the most complex allocation scenario. Throughput generally increases with more ONUs, as network resources (allocated subcarriers and timeslots) are utilized more efficiently. Fast tuning achieves the highest throughput since ONUs can freely switch subcarrier blocks without blocking. Fixed tuning results in the lowest throughput because ONUs remain restricted to the same block across frames. In slow tuning, throughput depends on the number of tuning frames, with better performance when fewer frames are required, as ONUs spend less time idle during tuning.

Figure 5 presents the throughput performance as a function of the number of subcarriers. Increasing the number of subcarriers allows the network to achieve higher throughput compared to the results shown in Fig. 3 and 4. To evaluate how the three tuning strategies perform with additional resources, we varied the number of subcarriers from 4 to 20, while keeping the offered load fixed at 1 and the number of ONUs fixed at 60. With more subcarriers, each ONU can potentially achieve a higher data rate, especially under high load conditions. However, in the fast tuning scenario, ONUs can freely switch between subcarrier blocks to satisfy their traffic demands, which results in the highest throughput as resources are fully utilized. In contrast, for the fixed tuning case, ONUs are restricted in their ability to switch blocks. Even with additional subcarriers, these ONUs can't fully take advantage of the extra resources, so the overall data rate does

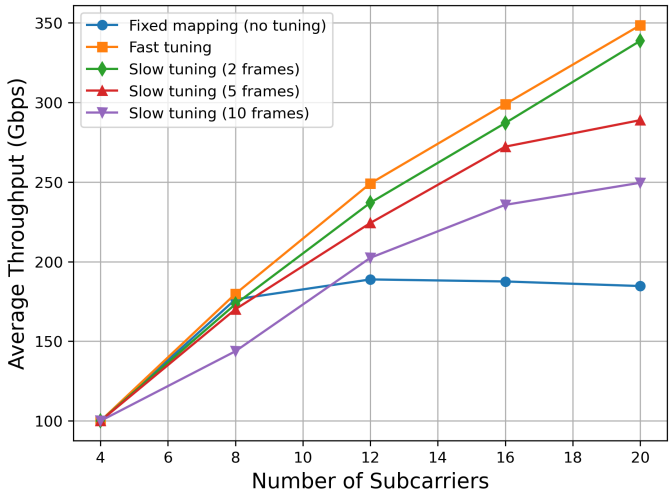

Fig. 5: Throughput as a function of number of subcarriers.

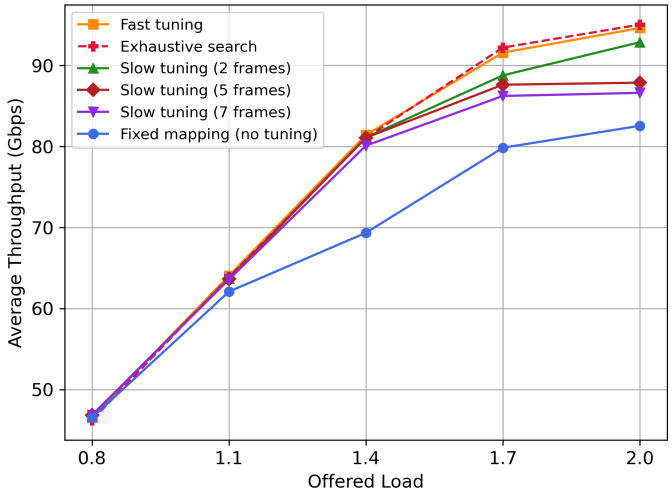

Fig. 6: Throughput as a function of load for small-scale.

not improve significantly.

To validate our heuristic, we implemented the optimal ILP solution for a small-scale scenario (e.g., 8 ONUs, 6 subcarriers) using exhaustive search. This explores all possible assignments, producing the optimal throughput. As shown in Fig. 6, the ILP optimality is very close to our proposed GGCA, slightly higher. This confirms that GGCA provides a near-optimal solution with much lower computational complexity. The computer which is employed for collecting simulation results had an Intel(R) Core(TM) i7-6700K central processing unit with random access memory of 16 GB.the exhaustive search takes around 2400 seconds to run for this small scale scenario, while GGCA achieves nearly the same throughput with much faster execution (e.g., 350 seconds) making it more practical for large-scale networks.

V. Conclusions

In this work, we proposed a greedy graph-based resource allocation algorithm for coherent optical access networks, where each ONU is assigned a block of adjacent subcarriers per frame. The algorithm efficiently allocates subcarriers and timeslots based on traffic demands, taking into consideration the mapping of the previous frame, to reduce the tuning operations among ONUs. Simulation results demonstrated that the proposed greedy allocation achieves significant performance improvements, particularly under high-load conditions, where fast tuning enables ONUs to utilize available resources more effectively compared to no-tuning and slow-tuning scenarios. Although this study focuses on the performance evaluation of throughput as a primary indicator, we plan to extend the performance evaluation to include latency-related metrics in our future work, such as end-to-end delay, jitter, and packet delay, which are critical for fronthaul and time-sensitive traffic.

Acknowledgment

This work has received funding from the European Union's Horizon Europe research and innovation programme under the Marie Skłodowska-Curie grant agreement No. 101073265 (EWOC). Views and opinions expressed are however those of the authors only and do not necessarily reflect those of the European Union. The European Union cannot be held responsible for them.

References

[1] ITU-T, "G.suppl.VHSP: PON transmission technologies above 50 Gb/s per wavelength."

[2] D. Nesset, "Progress on very high speed PON in ITU-T," in *2025 Optical Fiber Communications Conference and Exhibition (OFC)*, pp. 1–3, 2025.

[3] Z. Vujicic, M. C. Santos, R. Méndez, B. Klaiqi, J. Rodriguez, X. Gelabert, M. A. Rahman, and R. Gaudino, "Toward virtualized optical-wireless heterogeneous networks," *IEEE Access*, vol. 12, pp. 87776–87806, 2024.

[4] P. Torres-Ferrera, F. Effenberger, M. S. Faruk, S. J. Savory, and R. Gaudino, "Overview of high-speed TDM-PON beyond 50 Gbps per wavelength using digital signal processing [invited tutorial]," *Journal of Optical Communications and Networking*, vol. 14, no. 12, pp. 982–996, 2022.

[5] H. Zhang, Z. Jia, L. A. Campos, and C. Knittle, "Experimental demonstration of rate-flexible coherent PON up to 300 Gb/s," *Journal of Lightwave Technology*, vol. 42, no. 16, pp. 5440–5449, 2024.

[6] Z. Jia, H. Zhang, K. Choutagunta, and L. A. Campos, "Coherent passive optical network: applications, technologies, and specification development [invited tutorial]," *Journal of Optical Communications and Networking*, vol. 17, no. 1, pp. A71–A86, 2025.

[7] CableLabs, "CPON architecture specification." https://www.cablelabs.com/specifications/CPON-SP-ARCH, 2025. Accessed: July 2025.

[8] J. Zhou, Z. Xing, H. Wang, K. Zhang, X. Chen, Q. Feng, K. Zheng, Y. Zhao, Z. Dong, T. Gui, Z. Ye, and L. Li, "Flexible coherent optical access: Architectures, algorithms, and demonstrations," *Journal of Lightwave Technology*, vol. 42, no. 4, pp. 1193–1202, 2024.

[9] H. Zhang and Z. Jia, "100G TFDM coherent PON featuring burst signal processing in digital subcarriers," in *ICC 2023 - IEEE International Conference on Communications*, pp. 3302–3307, 2023.

[10] A. Kosowski and Kuszner, "On greedy graph coloring in the distributed model," in *Euro-Par 2006 Parallel Processing*, pp. 592–601, 2006.

[11] A. H. El Fawal, A. Mansour, and A. Nasser, "Markov-modulated poisson process modeling for machine-to-machine heterogeneous traffic," *Applied Sciences*, vol. 14, no. 18, 2024.

[12] S. Arnaout, M. A. Rahman, M. M. Mowla, S. Hausman, and P. Korbel, "Greedy graph coloring and hungarian algorithms for resource scheduling in TWDM-PON," *IEEE Access*, vol. 12, pp. 190400–190410, 2024.